Multiple porphyry events at Cerro de Pasco, central Peru

Conference Paper · August 2015

6 authors, including:

Bertrand Rottier
Laval University

Kalin Kouzmanov
University of Geneva

Vincent Casanova
University of Geneva

Multiple porphyry events at Cerro de Pasco, central Peru

Bertrand Rottier, Kalin Kouzmanov, Vincent Casanova and Lluís Fontboté
*University of Geneva, CH-1205 Geneva, Switzerland (*correspondence: Bertrand.Rottier@unige.ch)*
Ronner Bendezú and David Cuellar
Volcan Compania Minera S.A.A., Av. Gregorio Escobedo 710, Lima

Abstract. Cerro de Pasco, part of the Miocene metallogenic belt of central Peru, is one of the largest known epithermal base metal deposits. The deposit formed along the eastern margin of a diatreme-dome complex emplaced in the Mid-Miocene. It is interpreted to represent the upper part of a porphyry Cu system but until now no evidence of porphyry mineralization has been found. We report the first evidence of multiple porphyry events at Cerro de Pasco. First, hornfels and magmatic clasts with typical A- and B-type quartz-molybdenite porphyry veins were found incorporated in a magmatic breccia, part of the diatreme-dome complex. In addition, direct evidence of porphyry-style mineralization at surface has been found in a silica-rich andesitic plug-like body crosscutting the diatreme-dome complex. The body is affected by a network of quartz-magnetite-chalcopyrite-pyrite veins. Petrography, SEM-CL imaging, mineral thermometry and fluid inclusion studies indicate that quartz-molybdenite porphyry veins are formed in high-temperature and pressure environment, up to 600°C and 1.4 kbar. Late quartz-magnetite-chalcopyrite-pyrite veining affecting the andesitic plug shares characteristics with shallow porphyry-style mineralization. These new observations suggest that Cerro de Pasco is a long-lived mineralized system, product of multiple overprinting mineralizing events.

Keywords. Deep porphyry, shallow porphyry, Cerro de Pasco, clasts.

1 1 Introduction

The Miocene epithermal base metal deposit of Cerro de Pasco located along the eastern margin of a diatreme-dome complex with the oldest dated rocks being 15.36 ± 0.03 Ma (Baumgartner et al. 2009). It is the second largest known epithermal base metal ("Cordilleran") deposit after Butte in Montana, USA. The link between this large epithermal base metal mineralization dated at 14.5-14.4 Ma ($^{40}Ar/^{39}Ar$ dating of alunite, Baumgartner et al. 2009) and a porphyry system been proposed by Baumgartner et al (2008), but not confirmed so far.

In this contribution, we report the first evidence of multiple porphyry events at Cerro de Pasco. Hornfels and magmatic clasts with typical A- and B-type quartz-molybdenite veins have been found incorporated in the diatreme-breccia dated at 15.36 ± 0.03 Ma (Baumgartner et al. 2009), intersected by holes drilled in the south-eastern part of the diatreme-dome complex and also in the E-W trending quartz-monzonite porphyry dykes (15.35 to 15.16 Ma in age; Baumgartner et al. 2009). Considering the geochronology of the systems established by Baumgartner et al. (2009), the porphyry Mo mineralization could have taken place around 1 m.y. prior to the epithermal base metal mineralization.

In addition, direct evidence of porphyry-style mineralization at surface has been found in the central part of the diatreme in a tiny outcrop (approximately 12 x 5 m) of a silica-rich andesitic plug-like body crosscutting the diatreme dome complex. The porphyritic andesite is affected by a network of quartz-magnetite-chalcopyrite-pyrite veins, up to 1 cm in thickness.

Based on alteration, mineralization style, textural features, and geological context, in the following sections we refer to these two porphyry-style mineralizations, occurring respectively as clasts and in the andesitic plug, as “deep” and “shallow” porphyries. The new field observations at Cerro de Pasco allow studying the link between these two porphyry events and the base metal epithermal mineralization.

2 Deep Mo porphyry

Around 20% of the hornfels and porphyritic clasts found in the diatreme breccia are crosscut by 1 to 15 mm thick A- and B-type quartz-molybdenite porphyry veins (Fig. 1A-B). The clasts are mostly fine-grained and a majority of them is affected by high-temperature K-alteration (K-feldspar-biotite-andalusite-albite) assemblage. In places, the clasts are overprinted by lower-temperature argillic alteration (kaolinite-dickite-(illite) assemblage).

The following two types of high-temperature veins have been observed in the clasts: Thin (1-2 mm) and irregular quartz veins *(A-type*, Fig. 1A). Quartz contains glassy melt inclusions as well as two distinct sets of solid inclusions: (i) K-feldspar, biotite and rutile (Fig. 1C) i.e, an assemblage typical of potassic alteration. (ii) Actinolite, pyroxene, titanite, apatite, assemblage pointing to sodic-calcic alteration. These thin quartz veins are sulfide-poor (around 1%), the main sulfides being molybdenite, pyrite, and chalcopyrite. SEM-CL imaging reveals a single highly luminescent porphyry-stage quartz generation, with subtle subrounded oscillatory growth zoning (Fig. 1B), typical of high temperature quartz (>500°C), which is crosscut by later epithermal-stage quartz (see below). Ti contents in the second type of quartz veins lie between 30 to 69 ppm (electron microprobe). Application of the Ti-in-quartz thermometer considering a pressure of 1kbar and a_{Ti}=1 yields temperatures of 480-550°C and 600-680°C, using the equations of Thomas et al. (2010) and Huang and Audétat (2012), respectively. The second type of high-temperature veins are up to 2 cm thick and regular (*B-type*, Fig. 1E) that crosscut the A-type veins. They are almost free of mineral inclusions and present scarce melt inclusions which are crystallized (Fig. 1G). SEM-CL imaging reveals a single quartz generation with euhedral oscillatory growth zoning (Fig. 1F). These veins are also sulfide-poor (<1%), with mainly pyrite and rare molybdenite.

Commonly A- and B-type veins are re-opened and/or crosscut by late epithermal veins consisting of pyrite, sphalerite with "chalcopyrite disease", galena, chalcopyrite and fahlore group minerals associated with dark luminescent quartz.

A-type quartz veins present two types of fluid inclusion assemblages (FIAs): 1) High-density CO_2-rich vapor-rich inclusions with 60 to 90 vol % vapor (Fig. 1D). These inclusions commonly have daughter crystals of anhydrite, hematite and opaque minerals. Microthermometry results on FIAs yield homogenization temperatures (T_h) between 380° and 525°C, salinities from 11.5 to 18.4 wt% NaCl equiv., CO_2 contents between 12 and 25 mol%, and densities from 0.4 to 0.6 g/cc (calculated with the Q2 software, Bakker and Brown 2003, and the equation of Duan et al., 1992). Estimated minimum entrapment pressure varies from 25 to 120 MPa (calculated using the ISOC software, Bakker and Brown 2003) Raman analyses of the liquid phase of this first type of fluid inclusions have shown presence of SO_4^{2-} in solution in addition to the presence of anhydrite as a daughter phase, indicative of a sulfur-rich fluid. 2) Late secondary liquid-dominated fluid inclusions with 15 to 20 vol % vapor are also present. Microthermometric results yield homogenization temperatures from 230° to 270°C, and salinities from 19 to 25.5 wt% NaCl equiv. In most FIAs final ice melting occurs in metastable absence of hydrohalite. In some fluid inclusions opaque daughter crystals are present. Such low-temperature fluid is most probably associated to the epithermal stage overprint.

B-type quartz veins host two distinct types of FIAs: 1) Hypersaline fluid inclusions containing liquid, 40 to 50 vol % vapor, halite, and an unidentified daughter mineral (Fig. 1H). In addition, these inclusions often contain hematite crystals. Homogenization temperature is > 600°C and final halite melting temperatures vary from 360° to 400°C, corresponding to salinities of 43.3 to 47.4 wt% NaCl equiv. Minor amounts of CO_2 have been detected by Raman. Minimum entrapment pressure for such inclusions is >125 MPa. 2) Low-density vapor inclusions are also present; however, microthermometric experiments could not be performed on them.

The observations above indicate that the porphyry mineralization found in the clasts from the diatreme breccia is formed at high temperature and pressure. The high-density vapor-dominated CO_2- and sulfur-rich fluids found in the A-type veins are uncommon for porphyry deposits and their presence is indicative of important depth of formation.

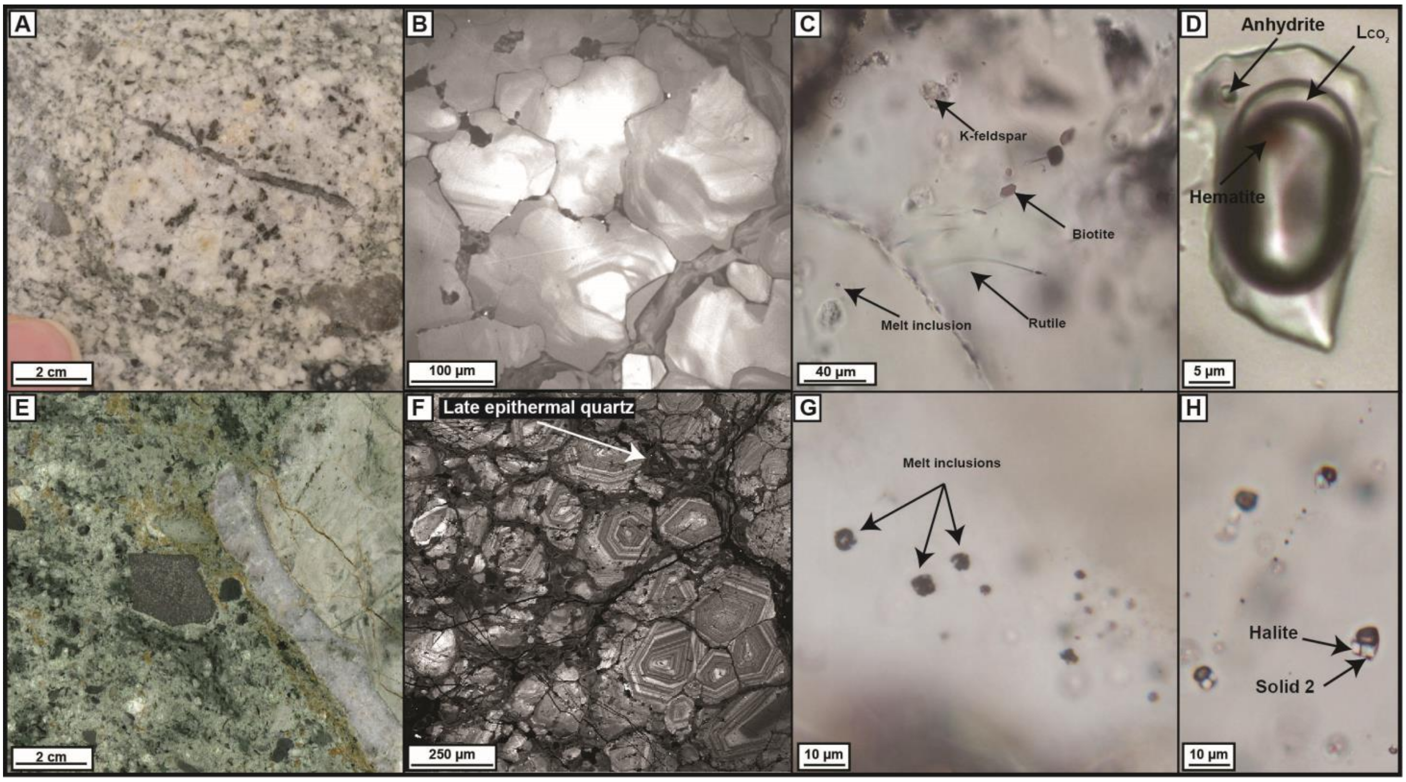

Figure 1. A) Porphyry clast with A-type quartz-molybdenite vein in the diatreme breccia; B) SEM-CL image of A-type quartz-molybdenite vein with subtle subrounded oscillatory growth zoning; C) Biotite, rutile and melt inclusions in quartz from A-type vein; D) High-density CO_2- and sulfur-rich vapor fluid inclusion from an A-type quartz-molybdenite vein; E) Hornfels clast with B-type quartz vein in the diatreme breccia; F) SEM-CL image of B-type quartz vein crosscut by late epithermal quartz; G) Crystallized primary melt inclusion assemblage in quartz from a B-type vein; H) Hypersaline fluid inclusions in quartz from a B-type vein.

3 Shallow Cu porphyry

The silica-rich andesite tiny plug is emplaced in the central part of the diatreme-dome complex. According to its geochemical features, it is the less evolved magmatic rock found in the Cerro de Pasco district so far. It crops out at the same elevation as the epithermal mineralization in the district. No indication of important erosion pre- or post-dating the epithermal stage of ore formation is recognized at Cerro de Pasco.

The plug is affected by pervasive chlorite-epidote-magnetite alteration spatially associated with a network of up to 2 cm thick quartz-magnetite-chalcopyrite-pyrite porphyry style veinlets (Fig. 2A). The veins are widespread and locally densely distributed, up to 20 veinlets per square meter. Microscopic observations reveal high chalcopyrite/pyrite ratios in the veins, with up to 5% chalcopyrite in some samples, both sulfides being affected by supergene oxidation. Quartz veins are banded in places (Fig. 2D) and SEM-Cl imaging reveals up to 3 different quartz generations (Fig. 2C): 1) High-luminescence resorbed euhedral sulfide-free quartz (Qz1) located along the vein borders. 2) High-luminescent sulfide-free quartz (Qz2) crosscuts the Qz1 generation. It forms botryoidal bands at the contact with Qz1, and becomes euhedral toward the center of the veins. In transmitted light, the botryoidal bands are dark gray, the color being due to abundant micron-sized vapor-rich fluid inclusions. This quartz probably recrystallized from a silica gel. 3) Late dark euhedral quartz (Qz3) crosscutting and overgrowing Qz1 and Qz2 and generally occurs in the center of the veins and between different bands of Qz1 and Qz2; it is commonly spatially associated with sulfides, mainly chalcopyrite.

Fluid inclusion petrography reveals a large number of vapor-rich inclusions occurring in the inner parts of the Qz1 crystals (Fig. 2E) and in bands in Qz2 (Fig. 2D). Liquid-rich fluid inclusions have been identified too. In addition, numerous hypersaline fluid inclusions, containing 30 to 50 vol % vapor, occur and show voluminous crystals of halite and of a second salt (sylvite?) representing up to 65% of the total volume, the liquid phase generally representing less than 10 volume percent (Fig. 2F). These hypersaline fluid inclusions also contain hematite and other opaque daughter crystals. They are generally hosted by Qz3 and could be associated with the sulfide precipitation.

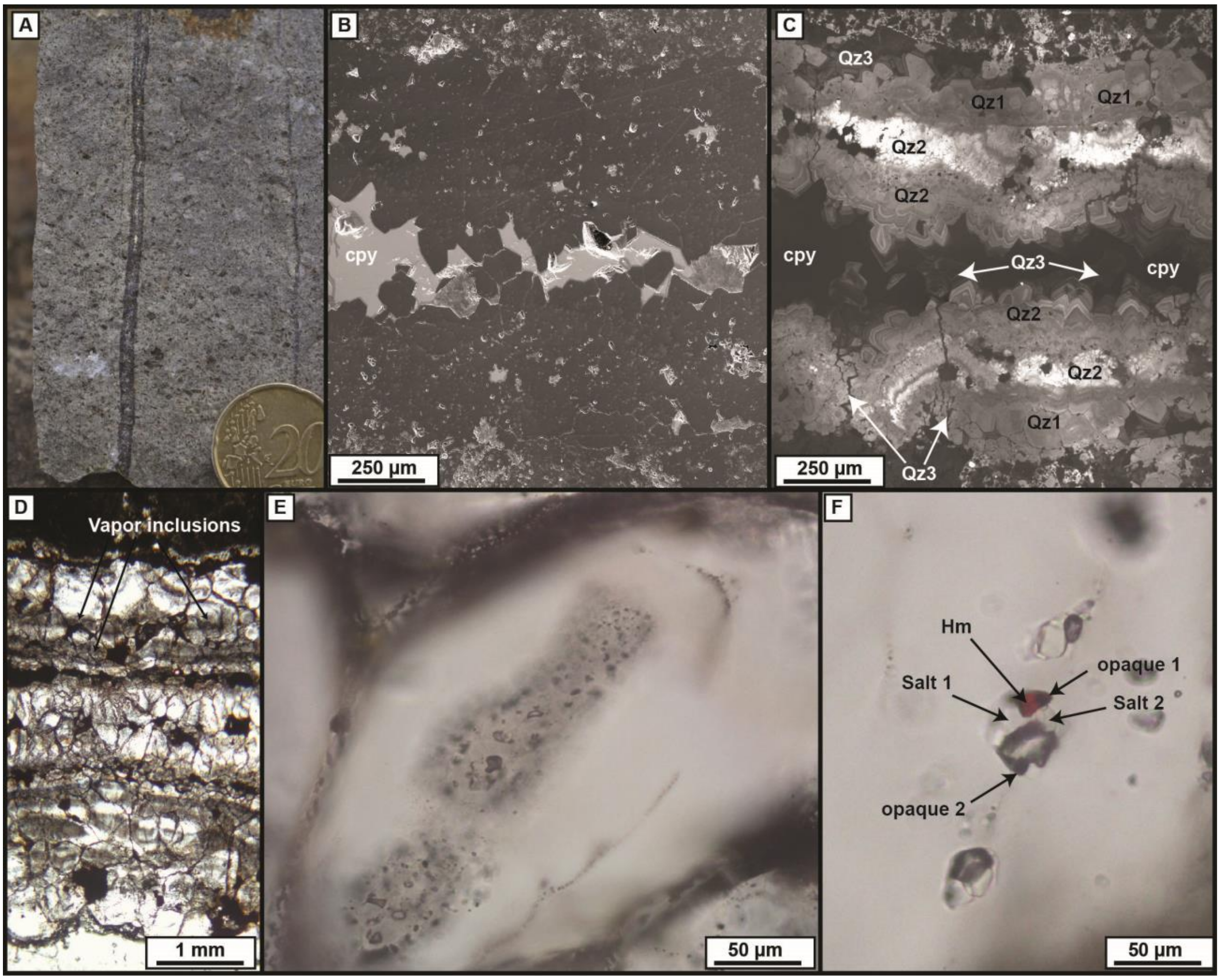

Figure 2. A) Quartz-magnetite-chalcopyrite-pyrite veins crosscutting the silica-rich andesite; B) BSE image of a quartz-magnetite-chalcopyrite-pyrite veinlet; C) Similar veinlet in SEM-CL showing textural relationships between different quartz generations; D) Banded quartz veins with dark bands outlined by vapor-rich fluid inclusions; E) Vapor-rich inclusions in the center of a Qz1; F) Hypersaline fluid inclusions in Qtz3.

The observed textures, crosscutting relationships with the host altered diatreme breccia and the fluid inclusion types are indicative of shallow emplacement of the porphyry plug. This interpretation is also coherent with the exposure of the porphyry plug at the same erosion level as the epithermal mineralization.

4 Cerro de Pasco long-lived porphyry centered magmatic-hydrothermal system

The new results highlight the complex history of Cerro de Pasco magmatic-hydrothermal system. The earliest hydrothermal event registered so far corresponds to the formation of the deep high-temperature quartz-Mo-Cu veins. These veins are then crosscut or re-opened by late epithermal lower-temperature quartz with a pyrite-sphalerite-galena-chalcopyrite-fahlore sulfide assemblage. Subsequently, parts of this mineralization have been incorporated as clasts in the diatreme-dome complex. Following the end of the magmatic activity, a large epithermal mineralizing event took place along the eastern margin of the diatreme-dome complex, resulting in the formation of both low sulfidation and high sulfidation base metals carbonate replacement ore bodies and high sulfidation base metal veins. The shallow high silica-rich andesite plug affected by a network of quartz-magnetite-chalcopyrite-pyrite porphyry style veinlets was emplaced in the central part of the system.

These observations enable to define Cerro de Pasco as long-lived porphyry centered magmatic-hydrothermal system formed by multiple contrasting in style mineralizing events. Long lived systems are commonly associated with telescoping between early high-T porphyry and late low-T epithermal environments (Sillitoe 1994) and with important uplift and erosion. However in the case of Cerro de Pasco, no important erosion is recognized after the emplacement of the base metal mineralization and of the shallow andesitic porphyry plug. Precise dating by ID-TIMS of magmaic zircons from a mineralized porphyry clast and from the silica-rich andesite plug to better constrain the timing of the two porphyry events is in progress.

Acknowledgements

This research is supported by the Swiss National Science Foundation (grant 200020_134872). The authors are grateful to the Volcan Compania Minera S.A.A. for the logistic support in the field.

References

Bakker R, and Brown P (2003) Computer modelling in fluid inclusion research. Mineral. Assoc. Can., Short Course ser. 32, 213-230.

Baumgartner R, Fontboté L, Vennemann T (2008) Mineral zoning and geochemistry of epithermal polymetallic Zn-Pb-Ag-Cu-Bi mineralization at Cerro de Pasco, Peru. Economic Geology 103: 493-537.

Baumgartner R, Fontboté L, Spikings R, Ovtcharova M, Schneider J, Pace L, Gutjahr M (2009) Bracketing the age of magmatichydrothermal activity at the Cerro de Pasco epithermal polymetallic deposit, central Peru: a U-Pb and 40Ar/39Ar study. Economic Geology 104: 479-504.

Duan Z, Møller N, Weare J (1992) An equation of state for the CH4-CO2-H2O system: II. Mixtures from 50 to 1000°C and 0 to 1000 bar. Geochimica et Cosmochimica Acta 56 : 2619–2631.

Huang R, and Audétat A (2012) The titanium-in-quartz (TitaniQ) thermobarometer: A critical examination and re-calibration: Geochimica et Cosmochimica Acta doi:10.1016/j.gca.2012.01.009.

Sillitoe R (1994) Erosion and collapse of volcanoes: Causes of telescoping in intrusion-centered ore deposits. Geoloy 22: 945-948.

Thomas J, Watson E, Spear S, Shemella T, Nayak K, Lanzirotti A (2010) TitaniQ under pressure: the effect of pressure and temperature on the solubility of Ti in quartz. Contributions to Mineralogy and Petrology 160: 743-759.